Available online at **www.joac.info**

ISSN: 2278-1862

Journal of Applicable Chemistry

2024, 13 (2): 59-72

(International Peer Reviewed Journal)

Quantitative Analysis of the Co-ordination Nature of the Synthesized Praseodymium(III) Isonicotinic acid Nanomaterial: Characterization and Study of Antimicrobial Properties

PunazungbaImsong, Juliana Sanchu,Sentienla Imsong, Mhasiriekho Ziekhrü and M.Indira Devi*

Department of Chemistry, Nagaland University, Lumami, Nagaland - 798627

Email: cam_indira@yahoo.co.in

Accepted on 10th March, 2024

ABSTRACT

Praseodymium (III): isonicotinic acid nano crystal was successfully synthesized through a simple technique and characterized by elemental analysis, molar conductance, FT-IR, X-ray powder diffraction, fluorescence, UV-Vis spectroscopy and the rmogravimetric studies. The evaluated Energy interaction and Judd Ofelt Intensity parameters from the UV-Vis spectra of the synthesized nano crystal could suggest the mode of co-ordination of Pr(III) with isonicotinic acid. Further, therein vitro antimicrobial properties were also studied. The isonicotinic acid ligand is composed of carbonyl oxygen atom and nitrogen atom of the pyridine ring as potential donor sites. Deprotonation of the ligand sites enabled metal-ligand coordination, and as a result, isonicotinic acid behaves as a bidentate ligand. A coordination number of nine was assigned to the praseodymium (III) ion in this nano crystal with monoclinic structure. The nanomaterial was found to be thermally stable and shows good photochemical and antimicrobial properties.

Graphical Abstract:

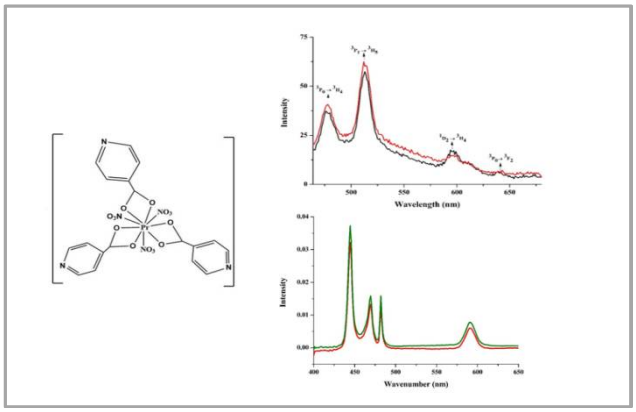

Synthesis, Characterization, and Functional Properties of Praseodymium(III): Isonicotinic Acid Nano Crystal with Enhanced Antimicrobial and Photochemical Attributes

Keywords: Pyridine, Praseodymium(III) nitrate hexahydrate, Antimicrobial activity.

INTRODUCTION

Over the last few decades, the domain of lanthanide chemistry has gained increasing prominence in the realm of modern science. These efforts focus largely on the creation of complexes with novel structural features for the production of advanced materials as well as the use of their unique spectroscopic properties in the development of biological probes and sensors in the fields of molecular biology and clinical chemistry. The wide range of applications for lanthanide compounds in biology and medicine has made lanthanide coordination chemistry an increasingly significant part of contemporary chemistry. The low toxicity and exceptional magnetic and luminous properties of lanthanide compounds make them particularly attractive for prospective uses [**1**] in medicine and diagnosis. There is a lot of interest in the interactions of rare earths with enzymes and proteins and their application as luminous probes in physiologically significant systems. Lanthanide ions have been commonly utilised as spectroscopic Ca^{2+} probes and as diagnostic tools in clinical research [**2**]. This is particularly notable due to the contrasting magnetic behaviours of calcium (diamagnetic) and praseodymium (paramagnetic). The bonding mechanism between the lanthanide and their ligands is extremely interesting and significant since their bio-applications involve the interaction of the biological ligands with the lanthanide [**3**].

Pyridine, an essential heterocyclic compound prevalent in many natural products, holds notable biological significance. The pyridine ring system serves as a vital component in numerous pharmaceuticals available in the market. Isonicotinic acid is a derivative of pyridine which has various applications in the synthesis of pharmaceuticals, agrochemicals, and coordination complexes due to its ability to form stable complexes with metal ions. It is often used as a ligand in coordination chemistry studies involving transition metals and lanthanides. As reported, lanthanides have demonstrated the capacity to create stable complexes with Schiff bases and many other newly synthesized compounds or its derivatives [**4**]. A significant percentage of these described nanomaterial have been utilised pharmaceutically. Lanthanide complexes have been reported to possess anticancer, antibacterial, antifungal, and several other diverse therapeutic characteristics [**5**]. Regarding biological efficacy, research indicates that lanthanide complexes exhibit enhanced antimicrobial activity contrast to the lanthanide ion and ligand [**6**].

The application of absorption spectrophotometry has proved to be a valuable and innovative approach for investigating lanthanide chemistry, especially in solution. This method offers a window into the complexities of f-electron transitions within various complexes, shedding light on their conformation and coordination environment. As a result, it has emerged as a robust tool for delving into the intricate chemistry of lanthanides.[**7-9**]. The power of the metal-ligand bond, coordination geometry, structure of the resulting complex, and interaction of chelate-solvent can be determined by the analysis of various transition states of *4f-4f spectra* of lanthanide ions [**10**].

In this study, it have successfully synthesized Praseodymium(III): Isonicotinic acid nano crystal through a facile method. The synthesized nanomaterial was characterized using the following techniques: elemental analysis, IR, powdered XRD, fluorescence studies, UV-Vis spectroscopy and TGA. UV-Vis absorption data was employed for computing the energy interaction and intensity parameters of Pr(III) and Pr(III):isonicotinic. This approach facilitated a theoretical exploration of the mode of binding of Pr(III) with isonicotinic acid. Molar conductance was measured, solubility and *in vitro* antimicrobial properties of the synthesized Pr(III): Isonicotinic acid complex was also further studied.

MATERIALS AND METHODS

Praseodymium(III) nitrate hexahydrate [$Pr(NO)_3.6H_2O$] of 99.9% purity was purchaed from Sigma Aesar and Isonicotinic acid ($C_6H_5NO_2$) was purchased from HIMEDIA. Various Agar were procured from HIMEDIA. Nutrient Broth and Sabouraud dextrose agar were purchased from HIMEDIA. The

percentage contents of C, H, O and N were estimatedemploying CHNS-Oanalyzer EuroVector. The metal content was determined by the oxalate-oxide method. Molar conductance with 10^{-3} M solutions of the sample is measured in a suitable solvent at room temperatures with Systronic direct reading conductometer. The IR spectra of the sample was runwith KBr pellets through spectrophotometer (Spectrum two) over the IR range. Luminescence analysis of the sample was done with SHIMADZU RF – 6000 spectrofluorometer. Powder X-Ray diffraction study was conducted with Rigaku Ultima IV diffractometer using $Cu_{k\alpha}$ radiation of wavelength λ = 1.5406 A from 10° to 80° (2θ) at room temperature. Thermal analysis was done using the SDT Q600V20.9 Build.

Synthesis of Pr(III) Isonicotinic acid complex: Praseodymium(III):Isonicotinic acid nanomaterial was synthesized using the general method outlined below. 20 ml of 0.01 mol aqueous solution of the ligand was added to 20 ml of hot alcoholic solution of praseodymium(III) nitrate hexahydrate and refluxed for 24-36 hours at its isoelectric point with a definite pH of the solution. The solution was then concentrated by keeping it in a water bath until its volume was reduced to half. After cooling, the solution underwent filtration;the residue got retained at normal temperature. Later on, the developed crystallite at the bottom of the beaker were collected and washed it with distilled water, alcohol and followed with ether. Collected crystals were then dried in a desiccator.

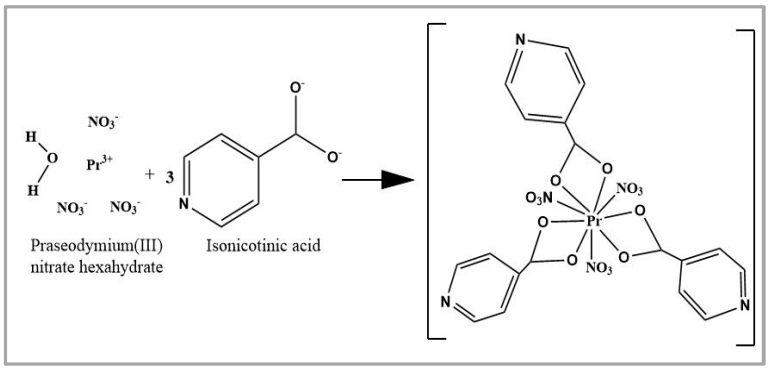

Figure 1. Probable chemical reaction for the synthesized Praseodymium(III):Isonicotinic acid nanocrystal.

Biological Activity

Source of Microorganism: For evaluating the antimicrobial effects, various isolates including Gram-positive bacteria like *Staphylococcus aureus* and *Bacillus subtilis*, as well as Gram-negative bacteria *Escherichia coli* and *Klebsiella pneumonia* were used. Additionally, fungal cultures like *Fusarium oxysposum*, *Penicillium italicum*, *Aspergillus niger* and *Candida albicans* were also involved in the study.

Antibacterial Assay: The antibacterial property of the synthesised nano crystal was evaluated focusing the zone of inhibition applying the well-diffusion method. Ampicillin was used as the standard drug for the antibacterial activity tests. The bacterial strains were cultured on 20 mL of sterile nutrient broth and incubated overnight at 37°C. The standard cultures were employed in a loop for the antibacterial test. Agar media was poured into the petri plates and left to solidify. The agar plate surface is used as the basal-medium for growth of the cultured bacteria. With the use of sterile borers, wells are made on the solidified agar media. The bacterial broth was spread uniformly on top of solid nutrient agar medium in petri plates. After air drying the inoculated agar medium, 50 µL of the sample with a 1 mg/mL concentration were loaded on to the bored wells and incubated for 24 h at 37°C. Reference antimicrobial drug is added to additional wells [**10**]. Following incubation, the clear zone of inhibition diameter (mm), formed around the centre of the well was measured and compared with the inhibition diameter of positive control ampicillin.

Following the same procedure of the antibacterial assessment, other antifungal tests were followed. Antifungal activity of the praseodymium complex was studied against four fungal strains, *Aspergillus niger, Penicillium italicum, Candida albicans* and *Fusarium oxysposum.* In contrast to the previous assay, Sabouraud dextrose agar was used instead of nutrient agar for media preparation. 50 µl of the specimen has beenput in the wells. The samples have been incubated at 30°C for 72 h. The resulting outcome have been recorded for the area of hinderance in mm [13].

Minimum Inhibitory Concentration (MIC): MIC has been found out employing the method of tube dilution with various dilution of sample (i.e., 300 µg mL^{-1}, 500 µg mL^{-1}, 600 µg mL^{-1}, 800 µg mL^{-1} and 1 mg mL^{-1}) [11]. These different concentrations of the sample were added into individual test tubes adjusting to 2 mL using nutrient broth. 2 mL of prepared solution taken in a test tube got autoclaved at 121°C with 15 lbs pressure for 15 minutes followed by sterilization. After cooling 0.2 mL of 24 h cultures for every bacterial strain were passed out into the antisepticintermediate and the further incubated for overnight. These actions are observed with examining the cloudiness in the stock [12].

RESULTS AND DISCUSSION

Analytical data indicates that praseodymium(III):Isonicotinic acid nanomaterial was formed with a metal-ligand stoichiometry of 1:3 and it possess good keeping qualities. The nano crystal is low water solubility solid and is soluble in methanol, ethanol, MeCN, DMF etc. Analytical values of the complex were found to be in conformation with their formation; elemental analysis and metal composition data which are given in table 1. The molar conductance value of the complex (Table 1) was in the range of 11.9 Ω cm^{-2} mol^{-1}in DMF solution at room temperature. This value implies that the nanocrystal doesn't form ions easily in nature [14].

Table 1. Analytical data of Praseodymium (III):Isonicotinic acid nanocrystal; calculated values are given in brackets

S. No.	Complex	%Yield	Colour	M	C	H	N	O	Molar conductance (DMF) Ω cm^{-2} mol^{-1}
1	$Pr(INA)_3(NO_3)_3$	91	Greenish	19.06 (19.01)	34.11 (34.16)	3.01 (2.96)	11.37 (11.46)	32.45 (32.40)	11.9

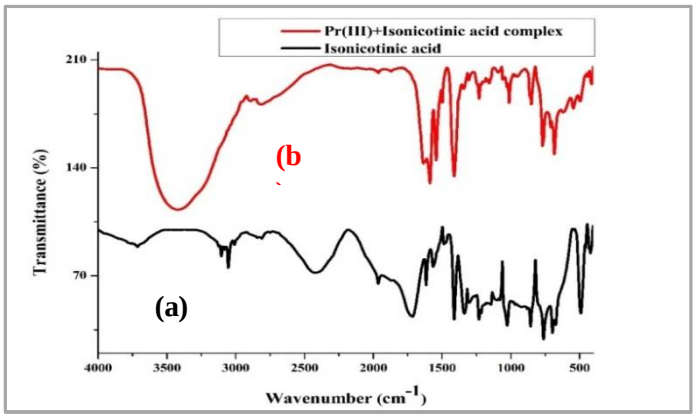

Figure 2. FT-IR spectra of (a) Isonicotinic acid and (b) Pr(III): Isonicotinic acid nanomaterial.

IR Spectra: The infrared spectra of Pr(III):Isonicotinic acid complex and pure ligand is shown in figure 2. The nature of infrared absorption frequencies of the synthesized nano complex in solid state are tabulated with table 2. On analysing the characteristic infrared absorption frequencies for the synthesize nano complex, we could observe intense peaks at 1644.98 cm^{-1} corresponding to the

asymmetric stretching vibrations of the carboxyl group as observed for the coordinated carboxylate ligands [15]. When a carboxylic acid is protonated, the stretching frequency shifts to 1700 cm^{-1} and when it is deprotonated the frequency shifts towards 1600 cm^{-1}. The -(C=O) vibration found in the IR spectrum for the complex at 1644.98 cm^{-1}got disappear in the spectrum of the ligand suggesting the deprotonation of the carboxyl group [**6**]. Electronic transition bands at 3414.92, 1231.62, 1021.06 and 690.70 cm^{-1}corresponded to -(C=N) and -(C=C) modes of the pyridine ring. C-H bending vibration becomes visible at 1409.47 cm^{-1}. The peaks in around 491.99 cm^{-1} and 419.62 cm^{-1} may correlate with metal coordination with oxygen and nitrogen sites; M-O and M-N, respectively [**16,17**]. Presence of asymmetric stretching vibration of -N-O was seen in 1539.49 which was absent in the ligand spectra.

Table 2. FT-IR wavenumbers with functional groups assigned to the Pr(III): Isonicotinic acid nanomaterial

S. No.	Assignments (Functional groups)	Wavenumber (cm^{-1})
		Pr(III):Isonicotinic acid complex
1	-HC=CH stretching (aromatic compound)	3414.92
2	-O-H (carboxylic acid)	2889.95(s), 2797.96(b)
3	-C=O (Carboxylic acid)	1644.98
4	-COO stretching	1589.78,
5	-N-O asymmetric stretching (nitro compound)	1539.49
6	-C-H bending (aromatic compound)	1409.47
7	-C-N stretching (aromatic compound)	1231.62
8	-CH=CH bending (aromatic compound)	1021.06, 690.70
9	Ring	851.38, 766.75

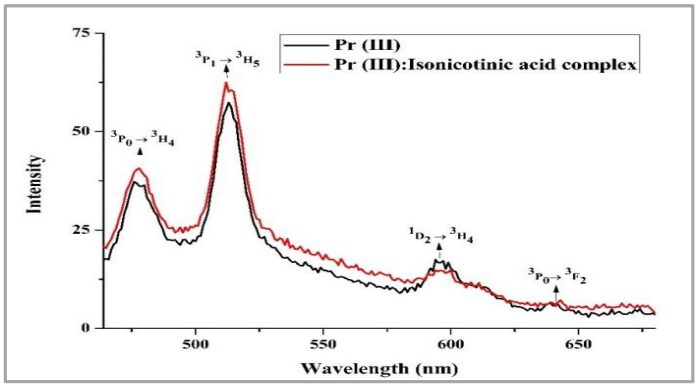

Figure 3. (a) Emission spectra of Pr(III) and Pr(III):Isonicotinic a cid nanocomplex.

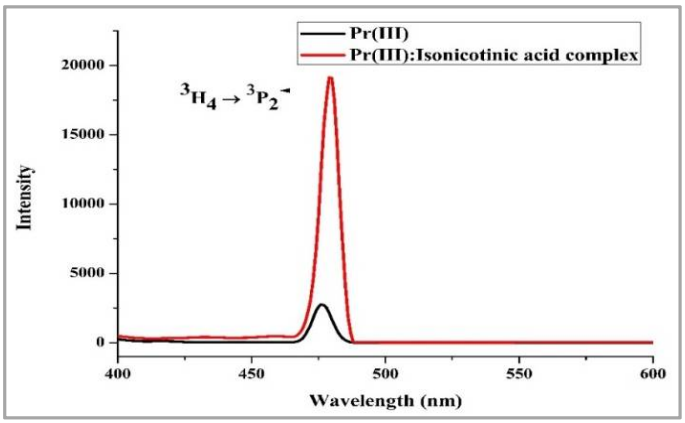

Figure 3. (b) Excitation spectra of Pr(III) and Pr(III):Isonicotinic acid nanocrystal.

Luminescence Studies: Figure 3 (a) and (b) shows the optical emission spectra of Pr^{3+} ion and Pr(III):Isonicotinic acid complex in the spectral region of 430–680 nm obtained by excitation at 444 nm corresponding to the $^3H_4 \rightarrow {}^3P_2$ transition of Pr(III). The emission bands centred at 477, 512, 595 and 640 nm are assigned to $^3P_0 \rightarrow {}^3H_4$, $^3P_1 \rightarrow {}^3H_5$, $^1D_2 \rightarrow {}^3H_4$ and $^3P_0 \rightarrow {}^3F_2$ transitions, respectively. Upon 444 nm excitation, the excited Pr^{3+} ion decays non-radiatively from the ^3P_J and $^1D_2$ excited state to the lower lying $^3H_4$, $^3H_5$ and $^3F_4$ energy states [**18, 19**]. The luminescence intensity of the emission transitions depends on the population of the complexes and Pr^{3+} ion in the excited levels. However, the intensity of the $^3P_0 \rightarrow {}^3H_4$ transition is high due to the fast non-radioactive decay from the higher lying $^3P_{2,1,0}$ levels. The inset of figure 3 describes the emission channels of Pr^{3+} ions in Pr(III): isonicotinic nano complex. From the emission spectra it is clear that the emission intensity of the $^3P_0 \rightarrow {}^3H_4$ transition is almost constant for the Pr(III):Isonicotinic acid complex due to the increase in the energy transfer among the excited Pr(III) ions. Moreover, the free metal ion and praseodymium(III) complex of the emission bands $^3P_0 \rightarrow {}^3F_4$ and $^1D_2 \rightarrow {}^3H_4$ transition overlap each other, whereas for $^3P_0 \rightarrow {}^3H_4$, $^3P_1 \rightarrow {}^3H_5$ are well resolved. Significant red shift has been observed for all the emission spectra; $^3P_0 \rightarrow {}^3H_4$, $^3P_1 \rightarrow {}^3H_5$, $^1D_2 \rightarrow {}^3H_4$ and $^3P_0 \rightarrow {}^3F_4$. The red shift associated could be due to the dispersion of excited ions in the surroundings of ligand fields during complexation [**20**] The intensities of all the observed emission bands increase on complexation to form nanocrystal. This may be mainly due to the phenomenon of quenching through drive between the excited states of Pr(III) ion. The discharge dominates from the $^3P_0$state which is populated by fast multiphonon non-radiative relaxation from the higher lying $^3P_{2,1,0}$ levels. As the interaction between Pr(III) ion and isonicotonic acid takes place, energy transfer process becomes more predominant and fast quenching in emission intensity takes place [**21**]. For Ln(III):Ligand complexes, red emission quenches significantly. The lanthanide nanocomplexes show distinct increase in the emission intensity compared to that of the free ionic form of the metal. Enhancement with the emission intensity associated with the complex shows clear evidence of metal-ligand complexation. The quantum yield for Pr(III):Isonicotinic acid nanocomplex was found to be 0.0575. Compared to the Pr(III) ion, which served as their precursor, the Pr(III) complex displayed significant fluorescence intensities. Binding of Pr(III) with ligand in the formation of the complex could have made the ligand more rigid in its conformation, which would have raised the fluorescence intensities of the complexes. These findings along with the value of quantum yield could indicate that the complex could be useful in photochemical applications [**22-24**].

X-Ray Diffraction: X-ray emissionmodel of Praseodymium(III):Isonicotinic acid nanocrystal is given in figure 4. Unit cell data and Miller indices were used to connect the Bragg angles and the set of interplanar spacing to these values, which were then applied to the individual reflections using the formula of sin 2θ [25]. The reflections between 2θ in the diffractogram of the complexes ranged from 10 to 80°, with a maxima at 2θ = 16.69.

The lattice parameters calculated for the unit cell value of Pr(III):Isonicotinic acid nanocrystal are; a = 7.2391 (Å), b = 7.4661 (Å), c = 6.3910 (Å) and cell volume of cell : 275.03 $(Å)^3$. The observed diffraction pattern corresponds to Anorthic crystal system which match with the JCPDS PDF No. 00-038-1885. The presence of possible phase such as PrO_3 is not observed. This confirms the possible lattice substitution of Pr^{3+}in $(C_6H_5NO)_3^-$ site. The crystallite size was estimated using the Scherrer formula:

$$d_{XRD} = \frac{\kappa\lambda}{\beta \cos\theta\prime}$$

where k is the shape factor (≈0.9), β is the full width at half maximum of the reflection peak, θ is Bragg's angle, and λ is the wavelength of Cu k_α radiation. The average crystallite size (d_{XRD}) is found to be 27.32 nm.

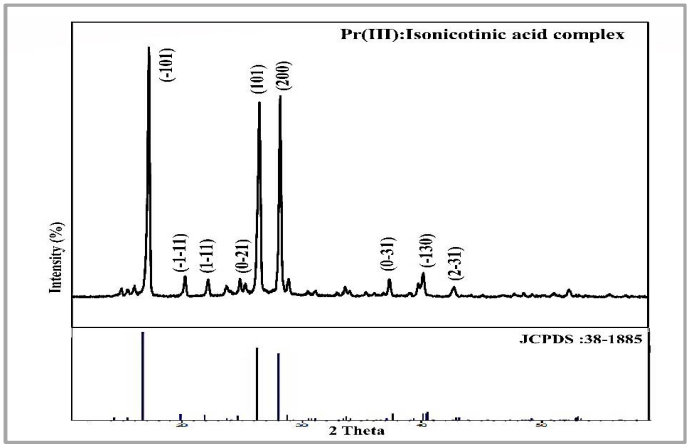

Figure 4. XRD spectrum of Praseodymium(III):Isonicotinic acid nanocrystal.

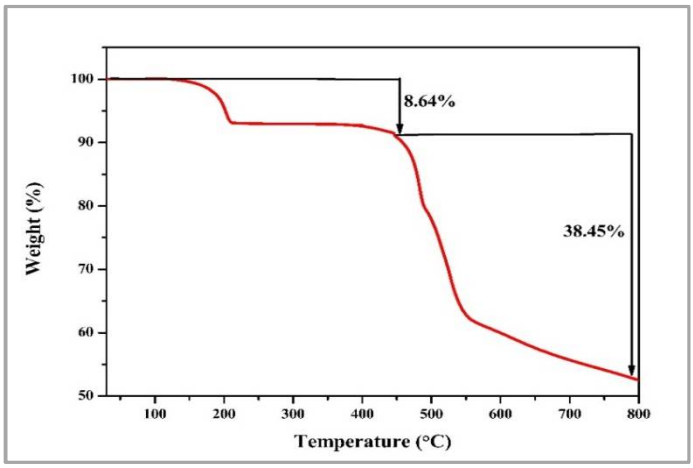

Figure 5. TGA of the synthesized Praseodymium(III): Isonicotinic acid nanocrystal.

Thermal analysis: The TGA measurements for Pr(III):Isonicotinic acid complex was done in dynamic air while being heated at a rate of 20°C min^{-1}. Figure 5 shows TGA curve associated with the complexfrom which it can be revealed that Praseodymium(III):Isonicotinic acid complex decomposes thermally in two stages; in the first stage a single molecule of pyridine decomposes and in the second stage two molecules of the Isonicotinic acid and methanoic acid was decomposed thus leaving $Pr(NO_3)_3$ as the final residue. The stages of decomposition were in good agreement when compared with the elemental analysis result. The praseodymium (III): Isonicotinic acid complex starts decomposition at a temperature higher than 470^oC which shows that the crystal is thermally stable at room temperature.

Antimicrobial activity

Antimicrobial Activity of Praseodymium(III) Complex: The antibacterial activity of Pr(III):Isonicotinic acid along with positive control commercial drug (Ampicillin) and negative control metal ion [**15**] were studied *in vitro* against four microbes organisms such as *Escherichia coli, Klebsiella pneumonia, Staphylococcus aureus* and *Bacillus subtilis. A*ntimicrobial accent of manufactured complex is show in table 3.Interestingly, the antimicrobial activity of Pr(III): Isonicotonic acid complex was found to be better than that of the reference drug ampicillin, as observed in the case of *Escherichia coli* and *Bacillus subtilis* while in the case of *Staphylococcus aureus* and *Klebsiella pneumonia* the activities were moderate in comparison to the reference drug. The zone of inhibition (mm) of Pr(III):Isonicotinic acid was 28 mm against *Escherichia coli* and 23

mm against *Bacillus subtilis* respectively. Negative control (metal ion) showed no zone of inhibition (Table 3).

Table 3. Antibacterial activity of Pr(III):Isonicotinic acid nanocrystal, metal ion as negative control, commercial drug as positive control.

S. No.	Name of bacterial pathogens	Zone of inhibition(mm)		
		Pr(III):Isonicotinic acid complex	Negative control	Positive control (Ampicillin)
1	*Escherichia coli*	28	No zone	25
2	*Klebsiella pneumonia*	21	No zone	28
3	*Staphylococcus aureus*	22	No zone	26
4	*Bacillus subtilis*	23	No zone	19

With reference to table 4 for the minimum inhibitory concentration of Pr(III)Isonicotinic acid, it is vividly seen that in the case of $Pr(Aspartic\ acid)_3(NO_3)_3$, the pathogen Escherichia coli growth is observed at 300 µg mL^{-1} and no growth in 500,600,800 µg mL^{-1} and 1mg mL^{-1}. Whereas in the case of $Pr(Histidine)_3(NO_3)_3$ and $Pr(Histidine)_3(NO_3)_3$, pathogen Escherichia coli growth is found at both 300 µg mL^{-1} and 500 µg mL^{-1} and no growth for the rest. Considering for the Bacillus subtilis, bacteria growth is found for 300 and 500 µg mL^{-1} in the case of $Pr(Aspartic\ acid)_3(NO_3)_3$, whereas for the case of $Pr(Histidine)_3(NO_3)_3$ and $Pr(Histidine)_3(NO_3)_3$ bacterial growth is at 300 µg mL^{-1} and no growth for the rest.

Table 4. Minimum Inhibitory Concentration of Pr(III):Isonicotinic acid complex against bacterial pathogens

S. No.	Name of the bacterial pathogens	Observation of Growth				
		300 µg mL^{-1}	500 µg mL^{-1}	600 µg mL^{-}	800 µg mL^{-1}	1 mg mL^{-1}
		$[Pr(Aspartic\ acid)_3(NO_3)_3]$				
1	*Escherichia coli*	+	-	-	-	-
2	*Bacillus subtilis*	+	+	-	-	-
		$[Pr(Histidine)_3(NO_3)_3]$				
1	*Escherichia coli*	+	+	-	-	-
2	*Bacillus subtilis*	+	-	-	-	-
		$[Pr(Valine)_3(NO_3)_3]$				
1	*Escherichia coli*	+	+	-	-	-
2	*Bacillus subtilis*	+	-	-	-	-

Note: + = Growth of bacteria, - = No growth of bacteria

The inhibitory activity of Pr(III):Isonicotinicacid nanomaterial was tested against four fungal pathogens; *Candida albicans*, *Aspergillus niger*, *Penicillium italicum*and *Fusarium oxysposum*. Among the fungal germs *Candida albicans* was highly venerable (38 mm) followed by *Aspergillus niger* (29 mm), *Penicillium italicum* (17 mm) and *Fusarium oxysposum* (14 mm). Antifungal outcomes are shown in table 5. The antimicrobial studies of confirm that the synthesized complex is biologically active. Overall, the complex exhibited very good antimicrobial activity against all of the tested pathogens.

Table 5. Antifungal Activity of Pr(III):Isonicotinic acid nanocrystal

S. No.	Name of Fungal Pathogens	Zone of inhibition (mm)
1	*Candida albicans*	38
2	*Aspergillus niger*	29
3	*Penicillium italicum*	17
4	*Fusarium oxysposum*	14

Minimum Inhibitory Concentration Assay: *Escherichia coli* and *Bacillus subtilis have been* examined to see the lowest level hampering obsession of microbes organisms and it has been found out *Bacillus subtilis at* 300 µg m L^{-1} and *Escherichia coli* at 500 µg m L^{-1} (Table 6, 7). These findings are in confirmation with that of Chohan *et al* [**26**].

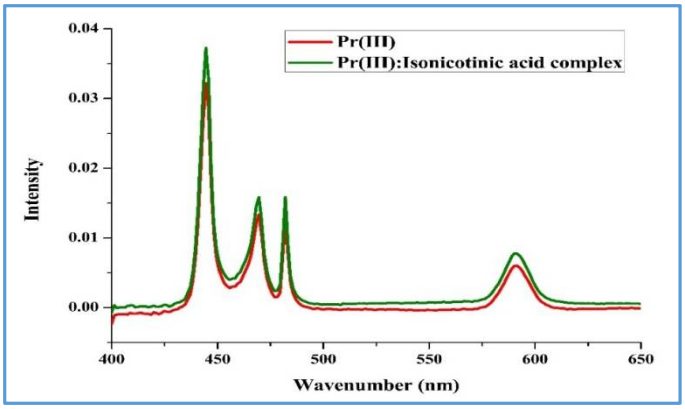

Figure 6. Absorption spectra of Pr(III) and Pr(III):Isonicotinic acid nanocrystal in aquated DMF (50%v/v).

Table 6. Computed value of energy interaction parameters Slater-Condon F_k(cm^{-1}), Spin Orbit Interaction ξ_{4f}(cm^{-1}), Nephelauxetic ratio (β), bonding ($b_{1/2}$), and covalency (δ) parameters of Pr(III) and Pr(III) with Isonicotinic acid in aquated(N,N Dimethylformamide) solvent.

System	F_2	F_4	F_6	ξ_{4f}	E_1	E_2	E_3	β	$b^{1/2}$	δ	RMS
DMF : Water											
Pr(III)	308.895	42.643	4.664	719.965	3507.395	23.735	614.104	0.944	0.166	5.856	122.50
Pr(III):Isonicotinic acid	308.592	42.601	4.649	719.767	3503.955	23.712	613.502	0.943	0.167	5.921	121.20

Table 7. Observed and calculated *P* and T_λ (T_λ, λ= 2, 4, 6) intensity parameter of Pr(III) with Isonicotinic acid in aquated Dimethylformamide solvent.

System	$^3H_4 \rightarrow {}^3P_2$		$^3H_4 \rightarrow {}^3P_1$		$^3H_4 \rightarrow {}^3P_0$		$^3H_4 \rightarrow {}^1D_2$		T_2	T_4	T_6
	Pobs	Pcal	Pobs	Pcal	Pobs	Pcal	Pobs	Pcal			
DMF: Water											
Pr(III)	5.355	5.355	1.826	1.288	0.739	1.270	0.915	0.915	-147.4	3.544	16.62
Pr(III):Isonicotinic acid	7.838	7.838	2.991	2.038	1.071	2.010	1.125	1.125	-265.5	5.614	24.24

The associated extensively comprehensive available internal f-electron along with susceptibility of Lanthanides to collaboration background and the shape of composite produced with different ligating molecules in simply available spectral regions have created a technique to an extensive means for employing absorption spectrophotometry as an important technique for analysing chemistry of lanthanides with solutions both in water and non-hygroscopicmedium [**27, 28**]. 4*f*-4*f* transitions spectra due to absorption by the Ln^{3+} ions are employed to evaluate the capability of coordination of Ln(III)incorporating suitable ligands, their resulting geometry, possible configuration of metal-ligand complex formed along with the mode of interaction as well as solvent-chelate [**29-31**].

Due to the presence of 4f electrons of lanthanide inside the deep core shell, they are naturally not vulnerable to the interaction background and their transitions are known as non-hypersensitive. Contrary to it, hypersensitive transitions obey the selection rule, $\Delta S = 0$, $\Delta L \leq 2$ and $\Delta J = \leq 2$ and are immensely susceptible to the variations of interaction background and consequently the strength of their band intensities becomes stronger when a lanthanide ions make complexation with suitable ligands [**32**].

These have been observed: transitions associated with Pr^{3+}, ($^3H_4 \rightarrow {}^3P_2$, $^3H_4 \rightarrow {}^3P_1$, $^3H_4 \rightarrow {}^3P_0$ and $^3H_4 \rightarrow {}^1D_2$) defy selection rules. But in some cases, their sensitivity associated with small variation in their coordination surroundings they could able to show uncommon sensitive nature. In fact, these transitions are pseudoquadrupole in nature and also named as Ligand Mediated Pseudohyper sensitive transitions which is because of the prompted outcome of their coordination surroundings. These Pseudohyper sensitive transitions have been employed considerably for the analysis of absorption spectrophotometry to comprehend the mode of binding, structural configurations of Pr(III) with various ligands in solution. The bindings of Pr(III) with various ligands and their susceptibility for making of complexes are displayed clearly by the associated increased intensity of the pseudo hypersensitive transitions [**33**]. In order to study the binding between Pr(III) ion and the Isonicotonic acid ligand, we have performed UV-Vis analysis on the free Pr^{3+} ion with the complex system in solution. Additionally, spectral parameters like the energy interaction and intensity parameters have been evaluated using UV-vis data to analyse theoretically the Pr(III) systems in solution.

Table 6 shows the computed values of the various parameters: Slator-Condon $F_k(k=2,4,6)$,Lande parameterξ_{4f}, Racah parameter E^k(k=1,2,3), Nephelauxetic ratio β, bonding parameter $b^{1/2}$,covalencyδ and RMS values. Getting through the variations of these data of Pr^{3+} and Pr(III):Isonicotinic acid complex in hydrated Dimethylformamide solutions, nature of bonding between Pr(III) and isonicotinic acid ligand could be studied. It could be revealed that the evaluated values of the inter-electronic repulsion parameters β, ξ_{4f} and $F_k$for the formation of Pr(III):Isonicotinic acid complex is less compared to that of the Pr(III) metal ion leading to the apparent making of complexes. The increase in inter-electronic binding parameters of percent covalency (δ) and the bonding parameter ($b^{1/2}$)followed by the nephelauxeticratio (β) values,(that was revealed below unity), could provide the probability of making covalent bond in the formation of complex of Pr^{3+} with isonicotinic acid. Reduced value of (β) could explain the extension of the central metal ion orbital thereby shortening the Pr^{3+} ligand bond distance known as nephelauxetic effect. The reduced values of *β could revealed* its association to the increase intensity of different electronic transition bands of Pr(III)($^3P_2$, $^3P_1$, $^3P_0$, and $^1D_2$) as shown in figure 7.6. RMS values could convey how far the evaluated values of energy interaction parameters are valid.

The intensity parameters: Judd-Ofelt parameters (T_λ) and Oscillator strength (P) for the ligand-mediated pseudohyper sensitive transitions ($^3H_4 \rightarrow {}^3P_2$, $^3H_4 \rightarrow {}^3P_1$, $^3H_4 \rightarrow {}^3P_0$, and $^3H_4 \rightarrow {}^1D_2$)for Pr^{3+}ion and Pr^{3+}:isonicotinic acid complex was evaluated (Table 7). The distinct variations of P (oscillator strength)values corresponding to*4f-4f* bands given in table 7. implies the propability of inner sphere coordination linking Pr(III) with isonicotinic acid. When Pr(III)interconnect with the ligand in solution, the magnitude of Judd-Ofelt parameter, T_λ (λ = 2, 4, 6) varies significantly; this validates the possible inner sphere binding of isonicotinic acid to Pr(III). The evaluated T_4 and T_6 parameters have been observed to be affected significantly on complexation and their values are found to be non-negative; hence, it may be employed in Judd-Ofelt theory for*4f-4f* transitions. T_4 and T_6 parameters are connected to variations in symmetry properties of the complex species hence, the distinct variation in the evaluated values of intensity parameters, T_4 and T_6could covey the propable variations in its nearest coordination environment thereby produces to the variations in the formation of complex Pr(III)with Isonicotinic acid. On other hand, $^3H_4 \rightarrow {}^3F_3$ transformation found on the other side of UV-Visible region hence, the evaluation of T_2 is non-positive accordingly, T_2 is neglected [**31, 34**]. Evaluation of Oscillator Strength P and its correlated T_λ have distinct changes; it could reveal the probability of inner-sphere complexation whereas minor variations of Oscillator Strength P and T_λ parameters could convey the possibility of outer-sphere complexation of Pr(III) with isonicotinic acid [**35**]. The distinct variations of evaluated P and T_λ values could convey possible proof of the association of isonicotinic acid with nona-inner-sphere coordination of Pr(III).

APPLICATION

The application for the synthesized Praseodymium(III): Isonicotinic acid nano crystal lies in its potential utilization in various fields including:

Catalysis: Due to its specific coordination structure and thermal stability, the nano crystal could serve as an effective catalyst in organic synthesis or industrial processes, where its unique properties could enhance reaction efficiency.

Photoluminescent Materials: The fluorescence properties of the nano crystal, as evaluated through fluorescence and UV-Vis spectroscopy, suggest potential applications in optoelectronic devices, such as LEDs or sensors, where its photochemical properties can be exploited.

Antimicrobial Agents: The in vitro antimicrobial properties indicate that this nano crystal could be explored as an antimicrobial agent in pharmaceuticals or biomedicine, offering a novel approach to combating microbial infections.

Drug Delivery Systems: The thermally stable nature of the nano crystal makes it a promising candidate for drug delivery systems, where controlled release of therapeutic agents can be achieved with minimal degradation or loss of activity.

Material Science: The characterization techniques employed, including elemental analysis, molar conductance, FT-IR, X-ray powder diffraction, provide valuable insights into the structural and chemical properties of the nano crystal, which can be leveraged in the development of advanced materials for various applications.

CONCLUSION

Pr(III):Isonicotinic acid nanocrystal was fruitfully manufactured and the it was further analyzed with different scientific methods. These complexes were found to be non-hygroscopic solid and soluble in water and most of the organic solvents. The molar conductance was found to be 11.9 $\Omega^{-1}cm^2mol^{-1}$ with DMF solution at normal temperature indicating the nanomaterial to be normal insulator. Praseodymium (III) was found to coordinate with Isonicotinic acid ligand via its oxygen anion of deprotonated carboxyl group and the nitrogen atom of the pyridine ring. The metal to oxygen and metal to nitrogen coordination have been justified by our IR data. The synthesized nanomaterial was crystalline in nature and they match the JCPDS PDF No. 00-038-1885 and average crystallite size (d_{XRD}) was calculated to be nano size of 27.32 nm. The lattice constants for the unit cell value of Pr (III): Isonicotinic acid complex are; a = 7.2391 (Å), b = 7.4661 (Å), c = 6.3910 (Å) and cell volume of cell: 275.03 $(Å)^3$. The synthesized complexes possess high thermal stability in air at normal temperature. Metal ion and the complex both are excited at 444 nm and the excited metal ion and complex decayed non-radioactively from the $^3P_1$ and $^1D_2$ excited state to the lower lying $^3H_4$, $^3H_5$ and $^3F_4$ energy states. The quantum yield was found to be 0.0575. The synthesized nanocrystal was found to exhibit good photochemical properties. The variation in the evaluated values of binding energy parameters (Slator-Condon $F_k(k=2,4,6)$,Lande parameterξ_{4f}, Racah parameter E^k(k=1,2,3), Nephelauxetic ratio β, bonding parameter $b^{1/2}$,covalencyδ) could reveal formation of complex between Pr(III) and isonicotinic acid. This fact is again substantiated with variations of values of oscillator strength (P) and Judd-Ofelt intensity parameters with the possible conclusion of formation of inner-sphere coordination between metal Pr(III) and ligand (Isonicotinic acid) with nona-coordinated structure. Based on the *in vitro* antimicrobial study, the synthesized complex was found to be biologically active and possess remarkable antimicrobial properties. Thus, such findings indicate that the synthesized nanocrystal could have potential photochemical and therapeutic applications.

ACKNOWLEDGMENT

The authors would like to acknowledge the department of Chemistry, Nagaland University; Lumami for providing the laboratory facilities. The authors are also grateful UGC NON-NET fellowship for the financial support.

Conflicts of Interest: The authors declare no conflicts of interest regarding the publication of this paper.

REFERENCES

[1]. L. R. Lin, H. H. Tang, Y. G. Wang, X. Wang, X. M. Fang, L. H. Ma, Functionalized Lanthanide(III) Complexes Constructed from Azobenzene Derivative and β-Diketone Ligands: Luminescent, Magnetic, and Reversible Trans-to-Cis Photoisomerization Properties, *Inorg. Chem.*, **2017**, 56, 3889–3900. https://doi.org/10.1021/ACS.INORGCHEM.6B02819/SUPPL_FILE/IC6B02819_SI_002.CIF.

[2]. C. H. Evans, Biochemistry of the Lanthanides, 1st ed., Springer, New York, **1990**. https://doi.org/10.1007/978-1-4684-8748-0.

[3]. C.H. Evans, The Interaction of Lanthanides with Amino Acids and Proteins, *Biochem. Lanthanides*., **1990**, 85–172. https://doi.org/10.1007/978-1-4684-8748-0_4.

[4]. E. Balogh, M. Mato-Iglesias, C. Platas-Iglesias, É. Tóth, K. Djanashvili, J.A. Peters, A. De Blas, T. Rodríguez-Blas, Pyridine- and phosphonate-containing ligands for stable Ln complexation. Extremely fast water exchange on the GdIII chelates, *Inorg. Chem.*, **2006**, 45, 8719–8728. https://doi.org/10.1021/ic0604157.

[5]. A. Ali Altaf, A. Shahzad, Z. Gul, N. Rasool, A. Badshah, B. Lal, E. Khan, E.A. Khan, A Review on the Medicinal Importance of Pyridine Derivatives, *J. Drug desing and Medicinal Chemistry*, **2015**, 1(1), 1-11. https://doi.org/10.11648/J.JDDMC. 20150101.11.

[6]. M. Nazir, I.I. Naqvi, M. Nazir, I.I. Naqvi, Synthesis, Spectral and Electrochemical Studies of Complex of Uranium(IV) with Pyridine-3-Carboxylic Acid, *Am. J. Anal. Chem*., **2013**, 4, 134–140. https://doi.org/10.4236/AJAC.2013.43018.

[7]. Z. Ahmed, K. Iftikhar, Synthesis and visible light luminescence of mononuclear nine-coordinate lanthanide complexes with 2,4,6-tris(2-pyridyl)-1,3,5-triazine, *Inorg. Chem. Commun.*, **2010**, 11, 1253–1258. https://doi.org/10.1016/J.INOCHE.2010.07.009.

[8]. Y.F. Zhao, H. Bin Chu, F. Bai, D.Q. Gao, H.X. Zhang, Y.S. Zhou, X.Y. Wei, M.N. Shan, H.Y. Li, Y.L. Zhao, Synthesis, crystal structure, luminescent property and antibacterial activity of lanthanide ternary complexes with 2,4,6-tri(2-pyridyl)-s-triazine, J. *Organomet. Chem*., **2012**, 716, 167–174.

[9]. L. Sorace, C. Benelli, D. Gatteschi, Lanthanides in molecular magnetism: old tools in a new field, *Chem. Soc. Rev.*, **2011**, 40, 3092–3104. https://doi.org/10.1039/C0CS00185F**.**

[10]. C. Sumitra, T. D. Singh, M.I. Devi, N.R. Singh, Absorption spectral studies of 4f-4f transitions for the complexation of Pr(III) and Nd(III) with glutathione reduced (GSH) in presence of Zn(II) in different aquated organic solvents and kinetics for the complexation of Pr(III):GSH with Zn(II), *J. Alloys Compd*., **2008**, 451, 365–371.

[11]. T. Balasankar, M. Gopalakrishnan, S. Nagarajan, Synthesis and antibacterial activity of some 5-(4-biphenylyl)-7-Aryl[3,4-d]-1,2,3-benzoselenadiazoles, **2008**, 22, 171–175. https://doi.org/10.1080/14756360601051365.

[12]. K. Mohanan, R. Aswathy, L.P. Nitha, N.E. Mathews, B.S. Kumari, Synthesis, spectroscopic characterization, DNA cleavage and antibacterial studies of a novel tridentate Schiff base and some lanthanide(III) complexes, *J. Rare Earths.*, **2014**, 32, 379–388. https://doi.org/10.1016/S1002-0721(14)60081-8.

[13]. M. S. Kadam, S. A. Khiste, S. A. Dake, B. C. Khade, Studies on X-Ray Diffraction, Thermogravimetric Stability, Antibacterial- Antifungal Activity of Fe(II), Ni(II), Cu(II) Metal Chloroquine Complexes Against Bacterial Strains and Fungal Spore, *Anti-Infective Agents*.,

2019, 18, 339–351. https://doi.org/10.2174/2211352517666191021090630.
[14]. W. J. Geary, The use of conductivity measurements in organic solvents for the characterisation of coordination compounds, *Coord. Chem. Rev.*, **1971**, 7, 81–122. https://doi.org/10.1016/S0010-8545(00)80009-0.
[15]. M. M. Omar, H. F. Abd El-Halim, E. A.M. Khalil, Synthesis, characterization, and biological and anticancer studies of mixed ligand complexes with Schiff base and 2,2′-bipyridine, *Appl. Organomet. Chem.*, **2017**, 31 e3724. https://doi.org/10.1002/AOC.3724.
[16]. P. P. Devi, F. A. S. Chipem, C. B. Singh, R. K. Lonibala, Complexation of 2-amino-3-(4-hydroxyphenyl)-N′-[(2-hydroxyphenyl) methylene] propane hydrazide with Mn(II), Co(II), Ni(II), Cu(II) and Zn(II) ions: Structural characterization, DFT, DNA binding and antimicrobial studies, J. Mol. Struct., **2019**, 1176 ,7–18. https://doi.org/10.1016/J.MOLSTRUC.2018.08.070.
[17]. M. Nazir, I.I. Naqvi, Synthesis and characterization of uranium (IV) complexes with various amino acids, *J. Saudi Chem. Soc.* **2010**, 14, 101–104. https://doi.org/10.1016/J.JSCS.2009.12.016.
[18]. A. Herrera, N.M. Balzaretti, Effect of High Pressure in the Luminescence of Pr^{3+} Doped Ge_2 O-PbO Glass Containing Au Nanoparticles, *J. Phys. Chem. C.*, **2018**, 122, 27829–27835. https://doi.org/10.1021/ACS.JPCC.8B08325/ASSET/IMAGES/MEDIUM/JP-2018-08325Q_0010.GIF.
[19]. C. Liu, F. Pan, Q. Peng, W. Zhou, R. Shi, L. Zhou, J. Zhang, J. Chen, H. Liang, Excitation wavelength dependent luminescence of LuNbO4:Pr3+-Influences of intervalence charge transfer and host sensitization, *J. Phys. Chem. C.* **2016**, 120, 26044–26053. https://doi.org/10.1021/ACS.JPCC.6B09806/SUPPL_FILE/JP6B09806_SI_001.PDf.
[20]. D. Rajesh, A. Balakrishna, M. Seshadri, Y.C. Ratnakaram, Spectroscopic investigations on Pr3+ and Nd3+ doped strontium–lithium–bismuth borate glasses, Spectrochim, *Acta Part A Mol. Biomol. Spectrosc*., **2012**, 97, 963–974. https://doi.org/10.1016/J.SAA.2012.07.100.
[21]. B. C. Jamalaiah, J. Suresh Kumar, A. Mohan Babu, L. Rama Moorthy, K. Jang, H. S. Lee, M. Jayasimhadri, J. H. Jeong, H. Choi, Optical absorption, fluorescence and decay properties of Pr^{3+}-doped $PbO–H_3BO_3–TiO_2–AlF_3$ glasses, *J. Lumin.*, **2009**, 129, 1023–1028. https://doi.org/10.1016/J.JLUMIN.2009.04.018.
[22]. C. Liu, W. Zhou, R. Shi, L. Lin, R. Zhou, J. Chen, Z. Li, H. Liang, Host-sensitized luminescence of Dy3+ in LuNbO4 under ultraviolet light and low-voltage electron beam excitation: energy transfer and white emission, *J. Mater. Chem. C.* **2017**, 5, 9012–9020. https://doi.org/10.1039/C7TC03260A.
[23]. R. Kamal, H. Hafez, Novel Down-converting single-phased white light Pr^{3+} doped $BaWO_4$ Nanophosphors material for DSSC applications, *Opt. Mater. (Amst).*, **2021**, 121, 111646. https://doi.org/10.1016/J.OPTMAT.2021.111646.
[24]. M. V Sasi Kumar, B. R. Reddy, S. Babu, A. Balakrishna, Y. C. Ratnakaram, B. Rajeswara Reddy, Thermal, structural and spectroscopic properties of Pr^{3+}-doped lead zinc borate glasses modified by alkali metal ions, **2018**, 11, 593–604. https://doi.org/10.1016/J.JTUSCI.2016.04.004.
[25]. S. Mathews, B. S. Kumari, G. Rijulal, K. Mohanan, Synthesis, Characterization and Antibacterial Activity of Some Transition Metal Complexes of 2-N-(isatinamino)-3-carboxyethyl-4,5,6,7-tetrahydrobenzo[b]thiophene, **2008**, 41, 154–161. https://doi.org/10.1080/00387010802007981.
[26]. Z. H. Chohan, C. T. Supuran, T. Ben Hadda, F. U. H. Nasim, K. M. Khan, Metal based isatin-derived sulfonamides: Their synthesis, characterization, coordination behavior and biological activity, **2009**, 24, 859–870. https://doi.org/10.1080/14756360802447636.
[27]. W.T. Carnall, P.R. Eieids, K. Rajnak, Electronic energy levels of the trivalent lanthanide aquo ions. II. $Gd^{3+,}$ *J. Chem. Phys.*, **1968**, 49, 4407–4411. https://doi.org/10.1063/1.1669894.
[28]. J.B. Gruber, G. W. Burdick, S. Chandra, D. K. Sardar, Analyses of the ultraviolet spectra of Er^{3+} in Er_2O_3 and Er^{3+} in Y_2O_3, *J. Appl. Phys.*, 2010, 108, 023109. https://doi.org/10.1063/1.3465615.
[29]. J. Sanchu, C. Imsong, Z. Thakro, D.M. Indira, Absorption spectral study for the interaction of

Pr(III) with L-Aspartic acid in various aquated organic solvents through 4f-4f transition spectra: Analysis of reaction pathways and thermodynamic parameters, *J. Pharm. Negat. Results*, 2022, 13(1), 860-878. https://doi.org/10.47750/PNR.2022.13.S01.105.

[30]. J. Sanchu, M. Ziekhrü, Z. Thakro, M. I. Devi, 4f-4f Transition Spectra of the Interaction of Pr(III) with L-Valine in Solution: Kinetics and Thermodynamic Studies, *Asian J. Chem.*, **2022**, 34, 2688–2696.

[31]. N. Bendangsenla, T. Moainla, J. Sanchu, M. I. Devi, Computation of Energy, Intensity and Thermodynamic Parameters for the Interaction of Ln(III) with Nucleic Acid: Analysis of Structural Conformations, Chemical Kinetics and Thermodynamic Behaviour through 4f-4f Transition Spectra as Probe, *J. Mater. Sci. Chem. Eng.*, **2018**, 6(7), 169-183. https://doi.org/10.4236/msce.2018.67018.

[32]. S. N. Misra, K. John, Difference and Comparative Absorption Spectra and Ligand Mediated Pseudohypersensitivity for 4f-4f Transitions of Pr (lll) and Nd (lll), **1993**, 28(4), 285-325. https://doi.org/10.1080/05704929308018115.

[33]. C. Klixbüll Jørgensen, B.R. Judd, C. Klixbüll Jørgensen, B.R. Judd, Hypersensitive pseudoquadrupole transitions in lanthanides, *MolPh.* **1964**, 8, 281–290. https://doi.org/10.1080/00268976400100321.

[34]. T. Moaienla, T. D. Singh, N. R. Singh, M. I. Devi, Computation of energy interaction parameters as well as electric dipole intensity parameters for the absorption spectral study of the interaction of Pr(III) with l-phenylalanine, l-glycine, l-alanine and l-aspartic acid in the presence and absence of Ca^{2+}, Spectrochim, *Acta - Part A Mol. Biomol. Spectrosc.*, **2009**, 74, 434–440. https://doi.org/10.1016/j.saa.2009.06.039

[35]. T. Moaienla, N. Bendangsenla, T. David Singh, C. Sumitra, N. Rajmuhon Singh, M. Indira Devi, Comparative 4f–4f absorption spectral study for the interactions of Nd(III) with some amino acids: Preliminary thermodynamics and kinetic studies of interaction of Nd(III):glycine with Ca(II), Spectrochim, *Acta Part A Mol. Biomol. Spectrosc.*, **2012**, 87, 142–150. https://doi.org/10.1016/J.SAA.2011.11.028.